CHAPTER IV

SUBCHRONIC EFFECTS OF THE CRUDE EXTRACT FROM *MUCUNA MACROCARPA* ON THE TILAPIA OVARY

INTRODUCTION

In contrast to the well documented reproductive effects of the extract from *Mucuna* species on the male reproductive system, although some *Mucuna* plants have been used at length in traditional medicine for treatment of gynecological disorders e.g. *M. pruritans* use in Ayurveda (Jadhav and Bhutani, 2005), study of their toxicological effects on female reproduction is still very limited. The black Kwao Krua, *Mucuna macrocarpa* Wall. (synonym: *Mucuna collettii* Lace) has been used in traditional Thai remedy for treatment of male sexual dysfunction. The study on its chemical constituents revealed 3 important compounds including kaempferol, quercetin and hopeaphenol (Roengsumran et al., 2001). Among many biological effects of these compounds documented, reproductive effects on female animals have been reported. Quercetin inhibits germinal vescicle breakdown and blocks fertilization in clam and starfish oocytes (Eckberg, 1983). Hopeaphenol is a tetramer of a well known phytoestrogen, resveratrol which exhibits variable degrees of estrogen receptor agonist (Gehm et al., 1997). The dietary treatment of resveratrol reduced body weight, disrupted estrous cycle and induced ovarian hypertrophy in normal adult female rats (Henry and Witt, 2002). Currently, there are 2 reports on *in vitro* effects of *M. macrocarpa* extract on human tumor cells indicating its antioxidant activity and mutagenicity (Sutjit, 2003) and cytotoxicity (Cherdshewasart, 2004). Study on

reproductive effect of powder-suspension *M. macrocarpa* in female rat revealed that the 1-month treatment at 10-100 mg/kg altered plasma sex hormone levels without histopathological alteration in the ovarian tissues (Thansa, 2003).

Subchronic toxicity is a toxicity due to exposure to quantities of a toxicant that do not cause any evident acute toxicity for a time period that is extended but is not so long as to constitute a significant part of the lifespan of the test species (Hodgson and Levi, 2000). A principal goal of the subchronic study is to identify and characterize the specific organ(s) affected by the test compound after repeated administration (Eaton and Klaassen, 2001). In reproductive toxicity study, subchronic assay is thus frequently assigned to assess the effects of the test chemical.

To elucidate the plant reproductive toxicity, we used subchronic toxicity bioassay to assess effects of *M. macrocarpa* crude extract on female Nile tilapia, *Oreochromis niloticus*. Changes in ovarian structure after exposure to plant extract were determined in the mature tilapia using histological methods for light and electron microscopy to examine reproductive morphological alterations at both cellular and subcellular levels.

MATERIALS AND METHODS

Fish procurement and maintenance

O. niloticus brood stock (3 weeks post-hatching) was obtained from the Aquatic Animal Breeding Research Station at Pathumtani, Department of Fisheries, the Ministry of Agriculture and Cooperatives of Thailand. The fish were raised in 325-L glass aquarium with aerated water. They were maintained on a 14 h light/10 h dark photoperiod at 27-29 °C and fed with commercial fish food (CP Company) twice daily. Water pH ranged between 6.6 and 7.5. The exposure began after fish reached 2 months of age in order to allow complete sex determination (Nakamura and Nakahama, 1985; Nakamura et al., 1993; Hines et al., 1999).

Preparation of M. macrocarpa crude extract

Whole stems and tubers of *M. macrocarpa* were ground and dried. The plant powder was extracted with absolute ethanol at room temperature for 2 weeks. Solvent extraction ratio was 1:10, powder (g): solvent (ml). The solution was filtered and the solvent was evaporated out by a rotary evaporator at 40°C at the Natural Products Research Unit, Department of Chemistry, Chulalongkorn University. The crude extract was dried in an oven at 40°C. The extraction process gave approximately 1.51% yield. All crude extracts yielded from each extraction process were pooled together before use in order to minimize variation in chemical composition between each batch.

Subchronic exposure

After the fish reached the age of 2 months, they were separated into 4 aquaria with 300 fish/aquarium. Two aquaria were assigned as the treatment group and the

remaining aquaria were assigned as the control and the solvent control groups. The treatment aquaria were filled with 200 litres of *M. macrocarpa* crude extract solution dissolved in dimethyl sulfoxide (DMSO) at the subchronic concentration of 14 ppm. The control aquarium was filled with 200 litres holding water, and solvent control aquarium was filled with 200 litres of DMSO solution at 20 ppm. The static renewal system was used throughout the experiment and the holding water of every aquarium was renewed every 4 days. The exposure was carried out continuously for seven months. During the exposure period, fish of every aquarium were sampled (n=20) every month from 4 to 7 months after exposure.

Gonadosomatic index (GSI)

After sampling, the fish were weighed and the ovaries were removed and weighed. The GSI was calculated as follows:

$$\text{Gonadosomatic index} = \frac{\text{Gonadal weight}}{\text{Body weight}} \times 100$$

The data of gonadosomatic index were collected and analyzed for difference between the control and the treated groups by Student's t-test using SPSS for Windows program (Chicago, IL).

Histology

The ovaries were fixed in 10% neutral buffered formalin and processed through standard histological technique for paraffin section (Humason, 1979). All tissue blocks were sectioned at 5 μm and stained with hematoxylin and eosin. Histological structure

and histopathological alterations in the ovaries were observed by light microscopy (Zeiss Axioskop 40) comparing between the control and the treated groups.

Ultrastructure

Sixteen ovaries (2 ovaries from control and 2 ovaries from treated groups of each sampling month) were sampled and fixed in 4% glutaraldehyde at 4 ^{o}C and post-fixed in 2% osmium tetroxide, and then processed through steps in the rapid protocol for TEM processing (Rowden and Lewis, 1974). Semi-thin sections (150-200 nm) were cut with an ultramicrotome (RMC MT-XL), stained with 0.5 % toluidine blue and observed by light microscopy. From 16 semi-thin samples, 8 samples were selected as representatives of every month and processed for thin sections. Thin sections (90-100 nm) were stained with lead citrate and uranyl acetate and were examined with transmission electron microscope (Jeol JEM-2010) at the Department of Biology, Boston University.

RESULTS

Gonadosomatic index

Gonadosomatic indices (GSI) of the control group were 0.83 ± 0.35, 0.84 ± 0.37, 0.37 ± 0.10 and 1.16 ± 0.5 after 4 to 7 months post-exposure. The GSI of the treated group were 2.67 ± 2.02, 1.28 ± 0.60, 1.55 ± 0.92 and 2.71 ± 1.45, respectively. There was no significant difference in GSI between the control and the treated groups at every sampling month (Figure 4-1).

Ovarian follicular organization

Fish in genus *Oreochromis* possesses a cystic type ovary with asynchronous follicular development. Cystovarian ovary is completely encased by the ovarian capsule and bears a true ovarian cavity, into which the ovigerous folds project (Connaughton and Aida, 1999). The ovary of *O. niloticus* in this study consisted of oocytes at different stages of development including 1) oogonial stage, 2) chromatin nucleolar stage, 3) perinucleolar stage, 4) cortical alveolar stage, 5) vitellogenic stage and 6) ripe (preovulatory) stage (West, 1990; Srijunngam and Wattanasirmkit, 2001).

Oogonial stage. Small spherical oogonia are grouped in a small cluster surrounded by thin connective tissue (Figure 4-2A). The oogonia possess a large homogeneous nucleus and a small volume of basophilic cytoplasm.

Chromatin nucleolar stage. The oocyte increases in size and possesses nucleus with large nucleolus and a small volume of basophilic cytoplasm (Figure 4-2A). At this stage, follicular wall was first observed as a thin layer of squamous cells.

Perinucleolar stage. The oocyte increases in size and possesses nucleus with perinuclear nucleoli and light eosinophilic cytoplasm (Figure 4-2B). The follicular wall

consists of two layers of somatic cells, the inner granulosa cells and the outer thecal cells. The perinucleolar oocyte is surrounded by a simple layer of flattened (squamous) or low cuboidal granulosa cells and an outer layer of simple or stratified thecal cells (Figure 4-3B). The granulosa cell of perinucleolar oocytes possesses an oval-shaped nucleus with heterochromatin and cytoplasm with a number of multivesicular bodies, rough endoplasmic reticulum and free ribosomes. Mitochondria are rarely seen at this stage. Interdigitation of cytoplasmic processes (microvilli) between the oocyte and granulosa cells is evident. Multivesicular bodies are found near the interdigitation area (Figure 4-11A). The thecal cell possesses an irregular-shaped nucleus with heterochromatin and cytoplasm with abundant globular smooth endoplasmic reticulum (Figure 4-13A).

Cortical alveolar stage. The oocyte increases in size and possesses a nucleus with the same character as the perinucleolar stage. The cytoplasm contains numerous cortical alveoli organized as a ring near the follicular wall (Figure 4-2C). The cortical alveolar oocyte is surrounded by a simple layer of cuboidal or low columnar granulosa cells and an outer layer of stratified thecal cells (Figure 4-3C). The two cell types are separated by a basement membrane which may be observed by electron microscopy. Vitelline envelope or *zona radiata* was observed at this stage as a layer of electron-dense amorphous material in the area of interdigitation of microvilli of the oocyte and the granulosa cells (Figure 4-3A). The granulosa cell of cortical alveolar oocyte possesses an irregular-shaped nucleus with heterochromatin and cytoplasm with well developed and dilated rough endoplasmic reticulum (Figure 4-11B). Electron-dense materials were found throughout the cytoplasm and in the area of vitelline envelope. A number of multivesicular bodies and free ribosomes are also evident. The thecal cell

possesses spherical nucleus with heterochromatin and relatively larger volume of cytoplasm containing round-oval mitochondria with tubulovesicular cristae, globular smooth endoplasmic reticulum and transport vesicles (Figure 4-13B).

Vitellogenic stage. The oocyte extensively increases in size due to deposition of yolk materials. The nucleus is relatively small compared to the amount of cytoplasm in which yolk and fat droplets deposit (Figure 4-2D). The deposited yolk granules were aggregated into large yolk droplets in late vitellogenic stage. The follicular wall is thin at early vitellogenic stage and becomes thicker at late vitellogenic stage (Figure 4-3D). The thickness of the follicular wall may be a result of yolk incorporation into granulosa cell layer and/or proliferation of the granulosa cells. The vitelline envelope also became thicker after entering the vitellogenic stage, forming a mesh pattern of electron-dense, homogeneous material (Figure 4-9C). Electron micrographs show that this pattern maybe a result of collective deposition of electron-dense material in the perivitelline space where the cytoplasmic processes of the oocyte and granulosa cells interdigitated. The proliferating granulosa cell of late vitellogenic oocyte possesses an irregular-shaped nucleus with heterochromatin and organelle-rich cytoplasm containing electron-dense material, mitochondria, free ribosomes, well developed and dilated tubular rough endoplasmic reticulum and a Golgi system (Figure 4-11C). The cisternae of rough endoplasmic reticulum are filled with an amorphous electron-lucent material. The thecal cells possess spherical homogeneous nucleus with peripheral clumps of heterochromatin and cytoplasm containing abundant round-oval mitochondria with tubulovesicular cristae, elongated mitochondria with lamellar cristae and globular smooth endoplasmic reticulum (Figure 4-13C).

Ripe stage. The oocyte is large and possesses eccentric nucleus (Figure 4-2E). The follicular wall is thin consisting of a simple layer of flattened granulosa cells and a simple layer of flattened thecal cells (Figure 4-3E). The vitelline envelope at this stage is relatively thicker than other stages. The granulosa cell of ripe oocyte also possesses a spherical nucleus with euchromatin and one large nucleolus and organelle-rich cytoplasm with numerous mitochondria, free ribosomes and well developed rough endoplasmic reticulum (Figure 4-11D). Mitochondria are elongate with electron-dense matrix. It was relatively difficult to observe thecal cell by electron microscopy at this stage because the follicular wall is very thin and the outermost layer is easily detached during the tissue processing.

Post-ovulatory follicle is the remaining structure of the ovulated follicle. The structure contains residual vitelline envelope and remaining follicular cells with macrophage infiltration (Figure 4-2F and 4-5F).

Ovarian histopathological alterations

Ovarian tissues of the control and the solvent control groups are normal at every month observed. The results from these control groups are presented as 'the control' in this study. The control group had ovaries in various stages ranging from immature ovaries containing oogonia and chromatin nucleolar oocytes, to maturing ovaries containing cortical alveolar and early vitellogenic oocytes, and mature ovaries with vitellogenic and ripe oocytes. These structurally normal maturing and mature ovaries were found in the control group from 4 to 7 months post-exposure. In the treated group at 4 months post-exposure, pyknosis and karyorhexis of oogonia were observed in an immature ovary containing only oocytes at oogonial stage (Figure 4-4F). But in the

mature ovary of the treated group, ovarian histological structures were normal with visible post-ovulatory follicles, the evidence of normal ovulation (Figure 4-5C-F). At 5 months post-exposure, a number of atretic vitellogenic follicles were found in mature ovaries of both control and treated fish (Figure 4-6). Follicular wall of vitellogenic oocyte of the control fish was normal with the evidence of yolk incorporation in the granulosa cell layer of the follicle (Figure 4-6E). However, hypertrophy of granulosa cell layer was observed in the follicular wall of vitellogenic oocytes of the treated fish (Figure 4-6F). There was a deposition of homogeneous eosinophilic material and fat droplets in the area of hypertrophy. At 6 months post-exposure, hypertrophy of granulosa cell layer was found to be more severe with a deposition of fat droplets, yolk and homogeneous eosinophilic material in the hypertrophied area (Figure 4-7F). Other histological characters of mature ovaries of both control and treated fish were normal with some atretic vitellogenic follicles (Figure 4-7A-E). At 7 months post-exposure, all mature ovaries contained ripe oocytes and some atretic vitellogenic follicles. Histological structures of these ovaries were normal (Figure 4-8A-D). The follicular wall of ripe oocytes in both control and treated groups were also normal with thin granulosa and thecal cell layers (Figure 4-8E-F).

Effects on ultrastructure of follicular wall

The vitelline envelope. The difference in structure of vitelline envelope was found between the ripe oocyte of the control and the treated fish. The vitelline envelope of the control oocyte was an electron-dense homogeneous mesh-pattern layer (Figure 4-9D). In the treated group, the vitelline envelope of the ripe oocyte consisted of an

additional layer of the less electron-dense amorphous material separated between the mesh-pattern layer and the granulosa cell bodies (Figure 4-10D).

The granulosa cells. The ultrastructure of granulosa cell of perinucleolar and cortical alveolar oocytes were not different between the control and the treated groups. They possessed a number of multivesicular bodies, well developed rough endoplasmic reticulum, free ribosomes, a few mitochondria and a deposition of electron-dense material in cortical alveolar oocyte (Figure 4-11A-B and 4-12A-B). In vitellogenic oocyte, hypertrophy of granulosa cell was observed in the treated group (Figure 4-12C). Nucleus and most of the organelles were packed at the periphery of this layer near the basement membrane. Structure of the mitochondria was normal. Rough endoplasmic reticulum was found in concentric whirling pattern (Figure 4-12C). Other area of the hypertrophied cytoplasm was filled with membranous debris, membrane-bounded vesicles, possibly autophagic vucuoles, and large fat droplets. In the treated ripe oocyte, the granulosa cell possessed only spherical mitochondria, some transport vesicles and some fat droplets (Figure 4-12D). Rough endoplasmic reticulum was rarely seen and free ribosomes were found in small amount.

The thecal cells. The thecal layer consists of two cell types, (a) squamous fibroblast-like thecal cell with poorly developed cytoplasm and (b) a larger thecal cell with organelle-rich cytoplasm. We focused our attention on the latter cell type, a special thecal cell, which is a steroid producing cell. In the control fish, special thecal cells showed abundant mitochondria with both tubular or tubulovesicular cristae and lamellar cristae, a globular smooth endoplasmic reticulum and transport vesicles with an electron-dense content (Figure 4-13). The thecal cells of perinucleolar and cortical alveolar oocytes had abundant globular smooth endoplasmic reticulum and some round-

oval mitochondria with tubulovesicular cristae and transport vesicles (Figure 4-13A-B). In the vitellogenic oocytes, both round-oval and elongated mitochondria with tubulovesicular and lamellar cristae were more abundant (Figure 4-13C). Globular smooth endoplasmic reticulum was also observed. In the treated group, the thecal cell of perinucleolar oocyte was active with abundant round-oval mitochondria with tubulovesicular cristae and abundant globular smooth endoplasmic reticulum (Figure 4-14A). But in cortical alveolar oocyte, the thecal cells had abundant myelin figures, dilated endoplasmic reticulum with an electron-lucent content and deposition of electron-dense material (Figure 4-14B). Mitochondria were rarely seen and a few isolated cisternae of rough endoplasmic reticulum were observed. In some cortical alveolar oocyte, the cytoplasm of thecal cell contained only myelin figures and dilated endoplasmic reticulum. In vitellogenic oocyte, the thecal cells showed elongated mitochondria with tubulovesicular and lamellar cristae, abundant globular smooth endoplasmic reticulum and transport vesicles (Figure 4-14C).

DISCUSSION

In this study, histological and ultrastructural endpoints were used to assess potential reproductive effects of *M. macrocarpa* crude extract on the female tilapia. Ovarian development based on gonadosomatic index was not significantly different between the control and the treated groups in any month examined.

Based on fish screening assay, GSI has been used as an indicator to assess the reproductive effects of chemicals on sexual development. Many of the hormonally active agents are among the test chemicals reported by fish screening assay. Similar to this study, the treatment of androgen (dihydrotestosterone) at 10-100 μg/l and anti-androgen (flutamide) at 100-1000 μg/l on adult female fathead minnows, *Pimephales promelas*, showed no significant effect on the GSI at every concentration, however, the treatment of aromatase inhibitor (fadrozole) at 25-100 μg/l caused significant reduction of the female GSI (Panter et al., 2004). The studies on effects of estrogenic chemicals on female fish also revealed the effect on the reduction of GSI. In long-term treatment of estrogen (17α-ethinylestradiol) on juvenile medaka, *Oryzias latipes*, 10-100 ng/l estrogen caused significant reduction of female GSI (Scholz and Gutzeit, 2000). The dietary treatment of 50-500 μg/kg estrogen (17β-estradiol) in adult female rainbow trout, *Salmo gairdneri*, also caused significant reduction of GSI (Billard and Richard, 1982).

Histological observation showed normal ovarian development in the control group. Mature ovaries with ripe oocytes, the latest stage of female germ cell, were found in both groups since 4 months post-exposure indicating complete oogenesis in both control and treated groups. Moreover, observation of the post-ovulatory follicles in these mature ovaries confirmed that there was ovulation occurred during this period. Major differences in ovarian histology found in the treated group were 1) pyknosis and

karyolysis of oogonia in the immature ovary, 2) ultrastructural alteration of thecal cells of the cortical alveolar oocytes, 3) hypertrophy of granulosa cell layer of the vitellogenic oocytes and 4) formation of abnormal layer of vitelline envelope of the ripe oocytes.

Death of germ cell is a normal phenomenon in developing gonad and it occurs in the ovary as apoptosis of oogonia and oocytes. Follicular atresia is apoptosis of the developing oocyte and their granulosa cells (Terranova and Taylor, 1999). Follicular atresia of vitellogenic oocytes had been found similarly in both control and treated groups in this study implying that germ cell apoptosis occurred normally at vitellogenic stage in the developing ovary of the tilapia. In contrast, pyknosis (condensed nucleus) and karyorhexis (fragmented nuclear material), the characters of apoptosis, found in the oogonia in the treated ovary may be accounted as an abnormal incidence since germ cell apoptosis in early oogenesis is unusual in fish (Higashino et al., 2002). Higashino et al. (2002) reported in the histological study of early oogenesis in barfin flounder, *Verasper moseri*, that apoptosis did not occur in any stage of early oogenesis in this fish or other fish species. Induction of germ cell apoptosis in the female tilapia exposed to the plant extract may involve with the activity of quercetin, one of the chemical compounds found in *M. macrocarpa* extract. This constituent has been reported to increase DNA fragmentation and caspase-3 activity in HPB-ALL cell line (Russo et al., 1999), enhance apoptotic DNA fragmentation in HL-60 and L1210 cell lines (Iwao and Tsukamoto, 1999), and inhibit DNA synthesis and induce apoptosis in regenerating liver after partial hepatectomy (Čipák et al., 2003).

Ultrastructural study revealed histopathological alterations in thecal cells of cortical alveolar oocytes of the treated fish. The cells possessed myelin figures and

dilated endoplasmic reticulum with an electron-lucent content instead of a typical composition of organelle in normal thecal cells of the oocyte at the same stage in the control fish. The presence of myelin figures, the concentric laminations of organellar membranes, is a character of cell injury occurred with dilation of endoplasmic reticulum (Kumar et al., 1992).

The hypertrophy of granulosa cells of vitellogenic oocyte in the treated group may be the result of abnormal accumulation of membrane-bounded vesicles and lipid droplets that was observed by electron microscopy. Abnormal intracellular accumulations suggest several potential scenarios including 1) a normal endogenous substance is produced at a normal or increased rate, but the metabolic rate to remove it is inadequate, or 2) a normal or abnormal endogenous substance has been accumulated because it cannot be metabolized, or 3) an abnormal exogenous substance has been deposited because the cell has neither the enzymatic machinery to degrade it nor the ability to transport it to other sites (Kumar et al., 1992). In this study, other organelles of the hypertrophied granulosa cell such as mitochondria and rough endoplasmic reticulum were still structurally intact. It implies that the lesion was reversible since there was no injury occurred with cellular organelles. Induction of granulosa cell hypertrophy during vitellogenic stage was also documented as the effect of carp pituitary fraction treatment in adult hypophysectomized catfish, *Heteropneustes fossilis*, however, it was discussed as an activation of the granulosa cells under gonadotrophin stimulation (Sundararaj et al., 1972). Hypertrophy of granulosa cells of vitellogenic oocyte was also reported in normal catfish, *Ictalurus nebulosus* (Rosenblum et al., 1987). In an ultrastructural study of ovarian follicle of *O. niloticus* by Nakamura et al. (1993), the vitellogenic oocyte of normal tilapia possesses hypertrophied granulosa cells,

but it was due to the development of organelles such as mitochondria and rough endoplasmic reticulum.

The possible cause of the formation of an amorphous material layer between the granulosa cell and the vitelline envelope is uncertain because the studies on ultrastructural differentiation during the process of oocyte expulsion from its follicle are limited. This incidence may be a result of cellular pathological alteration or possibly a process of disintegration of the oocyte and its follicle during ovulation. In some teleost, ovulation is due to hydration of the oocyte. In most cases, the process involves the appearance of a hole in the follicle and the production of coelomic fluid (Scott, 1987).

In long-term study on the effects of estrogen (17α-ethinylestradiol) on female medaka, *Oryzias latipes*, the females exposed to low concentration of estrogen at 10 ng/l since 5 day post-hatch had poor reproductive success but histological observation showed normal ovarian development and normal oogenesis (Balch et al., 2004). The mature ovaries of the treated medaka were similar to the control containing late vitellogenic oocytes and post-ovulatory follicles. The different result was observed in the dietary treatment of 50-500 μg/kg estrogen (17β-estradiol) in adult female rainbow trout, *Salmo gairdneri*, that vitellogenesis was inhibited and the ovaries remained at the previtellogenic stage with apparently normal oocytes and oogonia (Billard and Richard, 1982). In chronic treatment with a phytoestrogen, resveratrol at 100 μM in 10% ethanol daily, ovarian hypertrophy and tumor were reported in the female rats (Henry and Witt, 2002). In the study of reproductive effects of *M. macrocarpa* on female rats by Thansa (2003), the 1-month treatment of powder suspension at 10-100 mg/kg increased estrogen levels in adult cyclic females and decreased LH levels in adult ovariectomized

females but there was no histopathological alteration observed in the ovary of the treated females.

The present study examined the effects of *M. macrocarpa*, a plant used in traditional remedy for treating male sexual dysfunction and containing several hormonally active ingredients. Overall results from subchronic treatment on female tilapia showed some histopathological alterations of ovarian tissues in the treated fish. The incidences that may be considered as major histopathological effects were observed at ultrastructural level in the follicular cells including an ultrastructural alteration in thecal cells of the cortical alveolar oocytes and hypertrophy of granulosa cells of the vitellogenic oocytes. However, the oogenic process was not altered from the treatment of the plant extract.

FIGURES

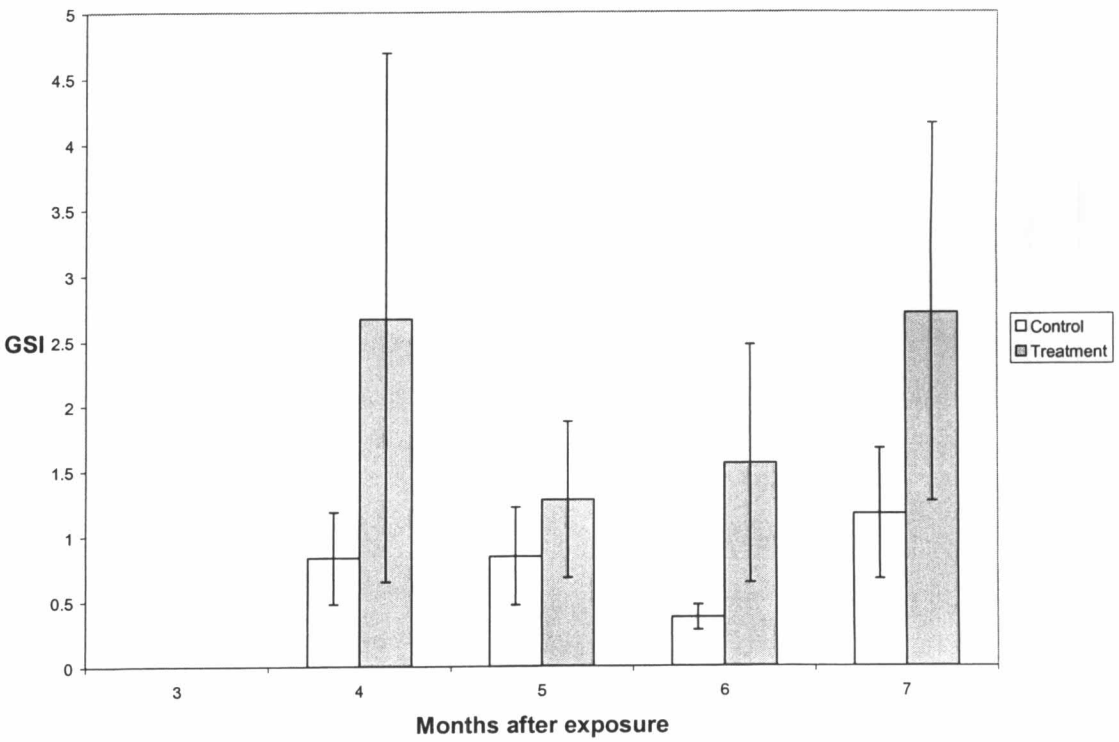

Figure 4-1: Gonadosomatic indices (GSI) of the female tilapia after 4 to 7 months of exposure (mean ± SE).

Figure 4-2: Oocytes of *O. niloticus* at different stages of development. (A) Oogonia in oogonial cyst and chromatin nucleolar oocyte contains nucleus with large nucleolus and basophilic cytoplasm. *Bar*: 20 μm. (B) Perinucleolar oocyte contains nucleus with numerous perinuclear nucleolus (arrow) and light eosinophilic cytoplasm. *Bar*: 20 μm. (C) Cortical alveolar oocyte contains numerous cortical alveoli (arrow) in the cytoplasm. *Bar*: 40 μm. (D) Vitellogenic oocyte contains cytoplasm with yolk droplets (arrow) deposition. *Bar*: 80 μm. (E) Ripe oocyte contains eccentric nucleus and cytoplasm with yolk materials. *Bar*: 150 μm. (F) Post-ovulatory follicle consists of residual *zona radiata* (*) and follicular wall cells (**). *Bar*: 80 μm.

Og oogonium, *C* chromatin nucleolar oocyte, *P* perinucleolar oocyte, *Ca* cortical alveolar oocyte, *V* vitellogenic oocyte, *R* ripe oocyte, *N* nucleus, *Pof* post-ovulatory follicle.

Figure 4-2

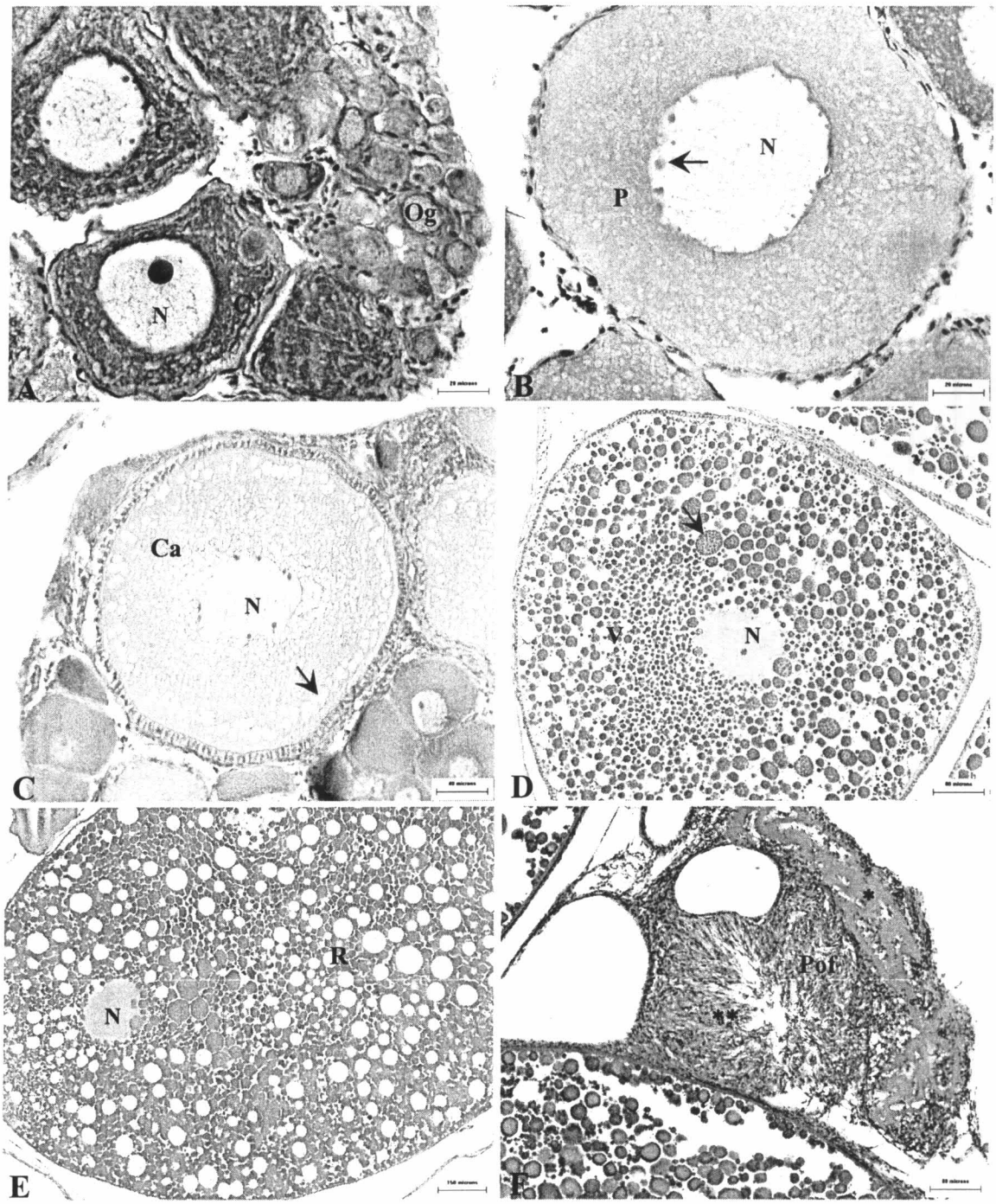

Figure 4-3: Ovarian follicles of *O. niloticus* at different stages of development. (A) Electron micrograph of follicle of cortical alveolar oocyte shows general composition of the follicular wall. *Bar*: 2 μm. (B) Follicle of perinucleolar oocyte comprises of thin granulosa and thecal cell layers. *Bar*: 20 μm. (C) Follicle of cortical alveolar oocyte comprises of columnar granulosa cell layer and thick thecal cell layer. *Bar*: 20 μm. (D) Follicles of early vitellogenic (left) and late vitellogenic oocytes (right) comprise of thick vitelline envelope and granulosa cell layer with yolk incorporation. *Bar*: 20 μm. (E) Follicle of ripe oocyte comprises of thick *zona radiata* and flattening granulosa and thecal cell layers. *Bar*: 20 μm.

Bm basement membrane, *G* granulosa cell, *T* thecal cell, *Ve* vitelline envelope.

Figure 4-3

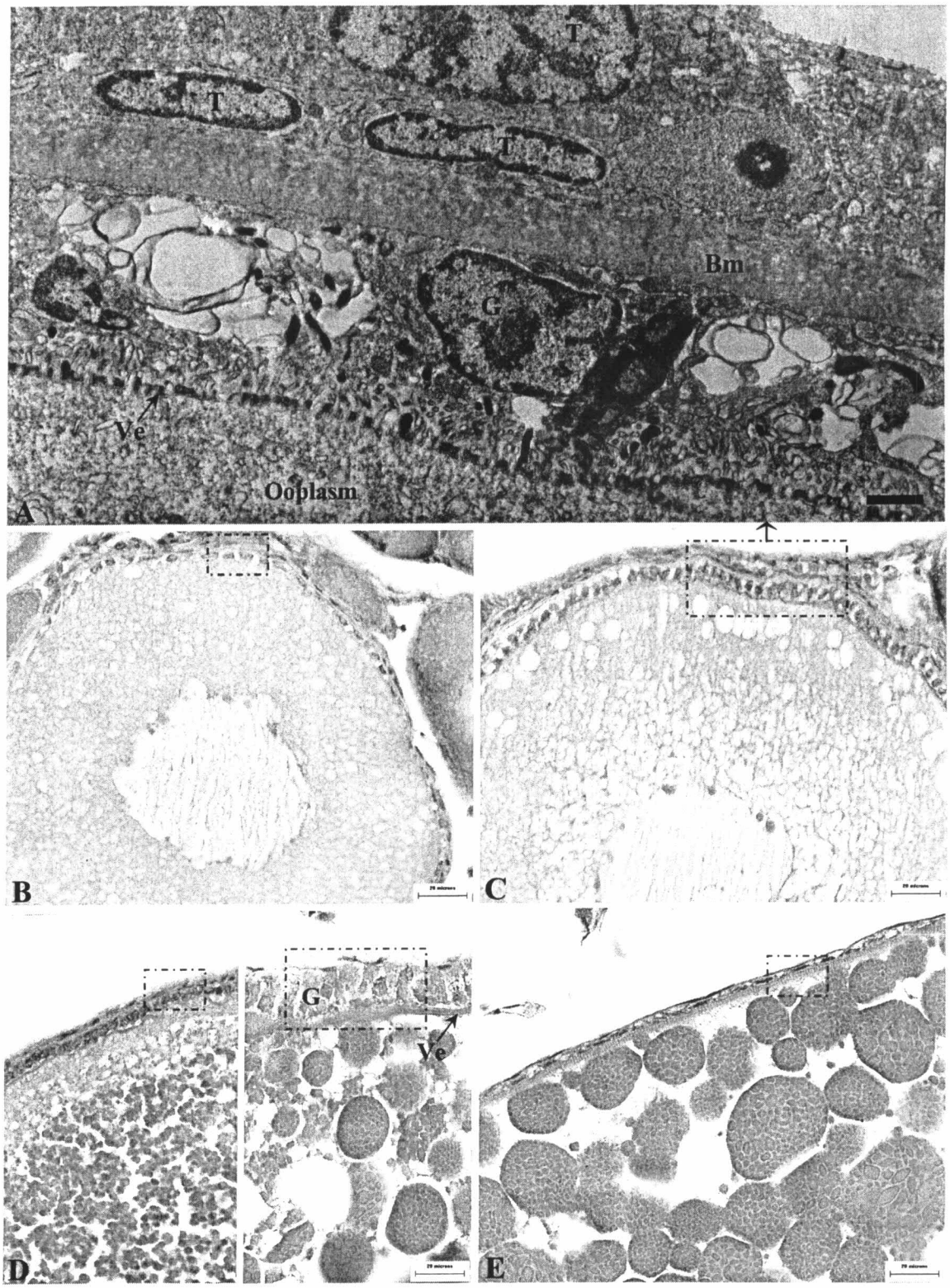

Figure 4-4: Ovaries of *O. niloticus* at 4 months post-exposure. (A-B) Maturing ovary of the control fish contains oocytes at different stages. *Bar*: 150 μm. (C-D) Immature ovary of the treated fish contains oogonia in the ovigerous folds (*). Large ovarian cavity is seen at this stage. *Bar*: 150 μm. (E) Control ovary shows chromatin nucleolar oocytes and oogonial cyst containing oogonia surrounded by interstitial tissue (*). *Bar*: 20 μm. (F) Oogonial cysts of the treated ovary with pyknosis of some oogonia (arrows). Inset shows karyorhexis of oogonia (arrow). *Bar*: 20 μm.

Og oogonium, *Oc* ovarian cavity, *C* chromatin nucleolar oocyte, *P* perinucleolar oocyte, *Ca* cortical alveolar oocyte, *V* vitellogenic oocyte.

Figure 4-4

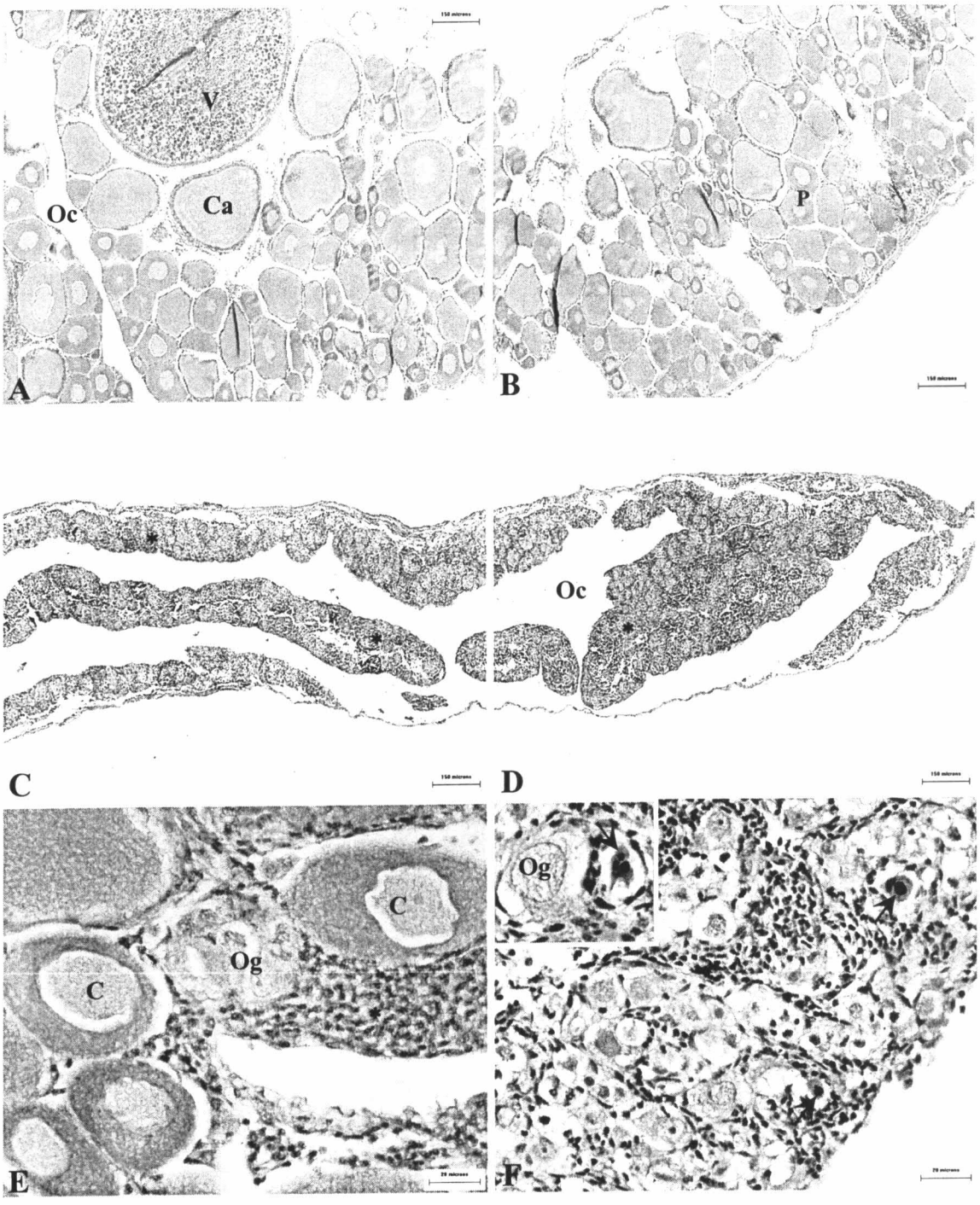

Figure 4-5: Mature ovaries of *O. niloticus* at 4 months post-exposure. (A-B) Control ovary contains ripe oocyte with eccentric nucleus (arrow) and other stages oocytes. *Bar*: 150 μm. (C-D) Treated ovary shows ripe oocytes and late vitellogenic oocyte. *Bar*: 150 μm. (E) Post-ovulatory follicle (arrow) found in the treated ovary. *Bar*: 150 μm. (F) High magnification of post-ovulatory follicle of the treated ovary shows remaining granulosa cell layer with long cytoplasmic processes (arrow). Macrophage (M) and residual vitelline envelope (*) are seen. *Bar*: 20 μm.

V vitellogenic oocyte, *R* ripe oocyte.

Figure 4-5

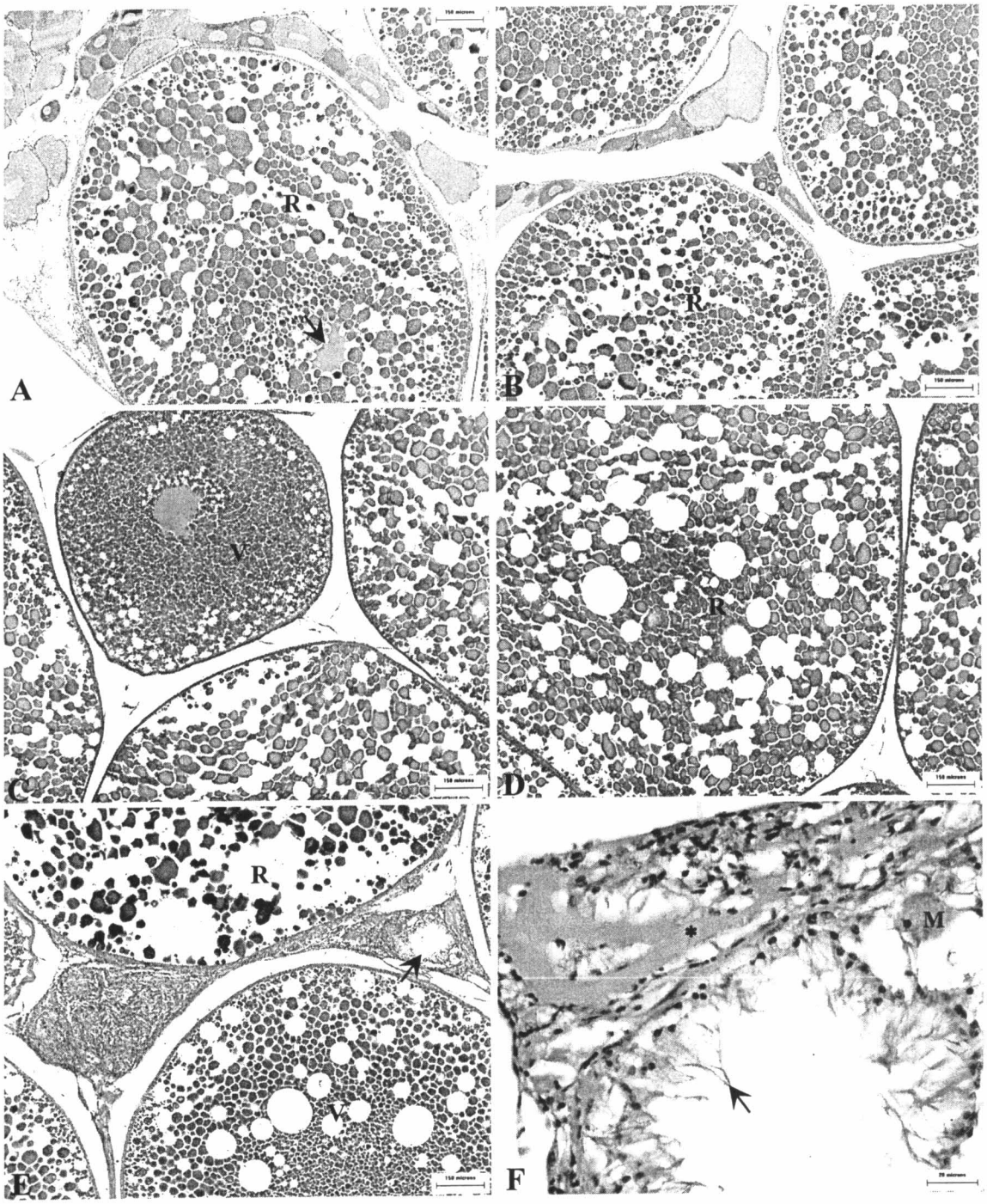

Figure 4-6: Mature ovaries of *O. niloticus* at 5 months post-exposure. (A-B) Control ovary contains ripe oocytes and atretic vitellogenic follicles (*). *Bar*: 150 μm. (C-D) Treated ovary contains large ripe oocytes with eccentric nucleus (arrow) and atretic vitellogenic follicle (*). *Bar*: 150 μm. (E) Ovarian follicle of the control fish shows normal granulosa cell layer with yolk incorporation (arrows). *Bar*: 20 μm. (F) Ovarian follicle of the treated fish shows hypertrophied granulosa cell layer with eosinophilic homogeneous material and large fat droplets (arrows). *Bar*: 20 μm.

V vitellogenic oocyte, *R* ripe oocyte, *G* granulosa cell.

Figure 4-6

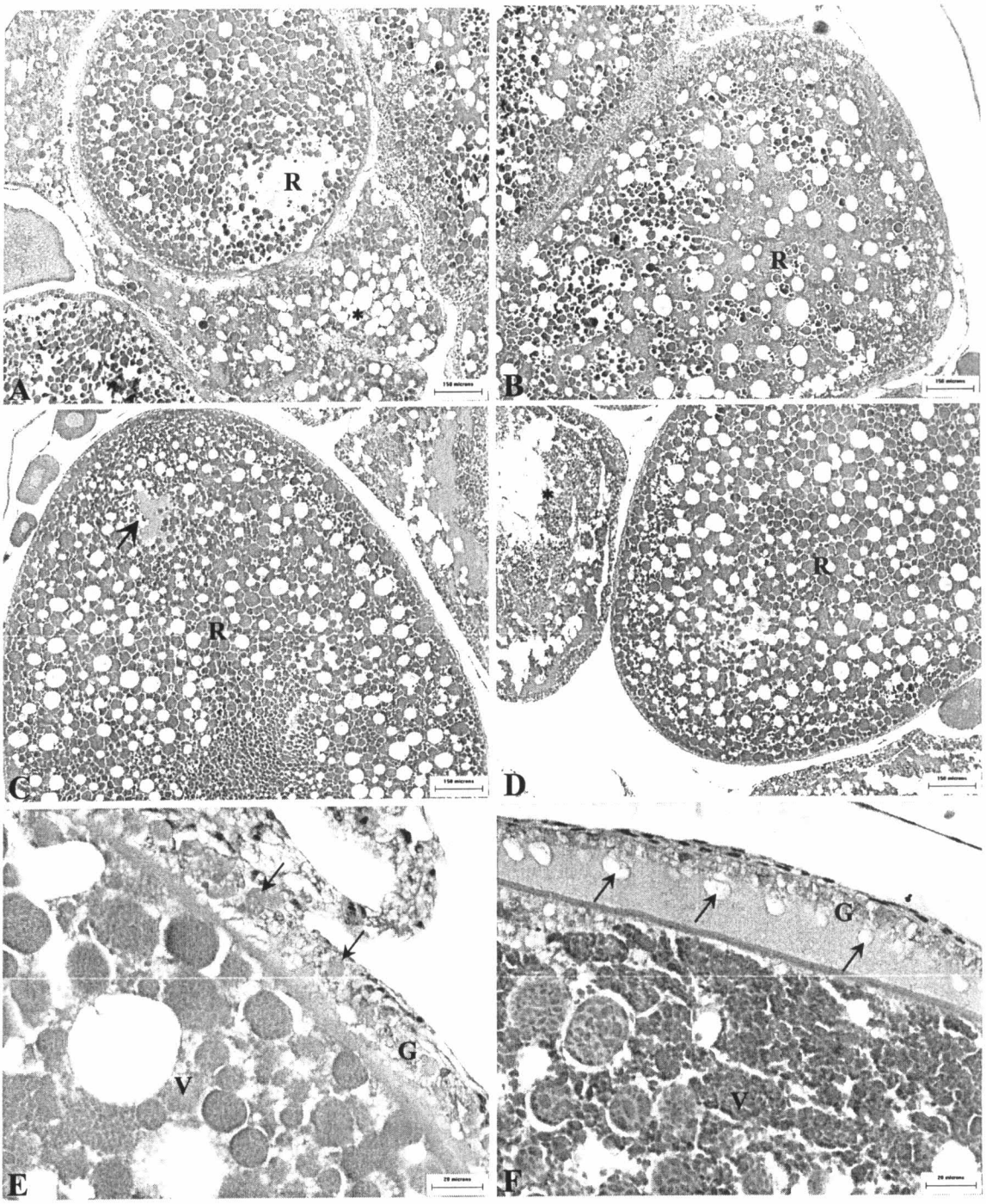

Figure 4-7: Mature ovaries of *O. niloticus* at 6 months post-exposure. (A-B) Control ovary shows ripe oocytes and atretic vitellogenic follicle (∗). *Bar*: 150 μm. (C-D) Treated ovary shows ripe oocytes and atretic vitellogenic follicle (∗). *Bar*: 150 μm. (E) Normal follicle of vitellogenic oocyte of the control fish. *Bar*: 20 μm. (F) Follicle of vitellogenic oocyte of the treated fish with severe hypertrophy resulting in extensive thickness of granulosa cell layer. *Bar*: 20 μm.

V vitellogenic oocyte, *R* ripe oocyte, *G* granulosa cell.

Figure 4-7

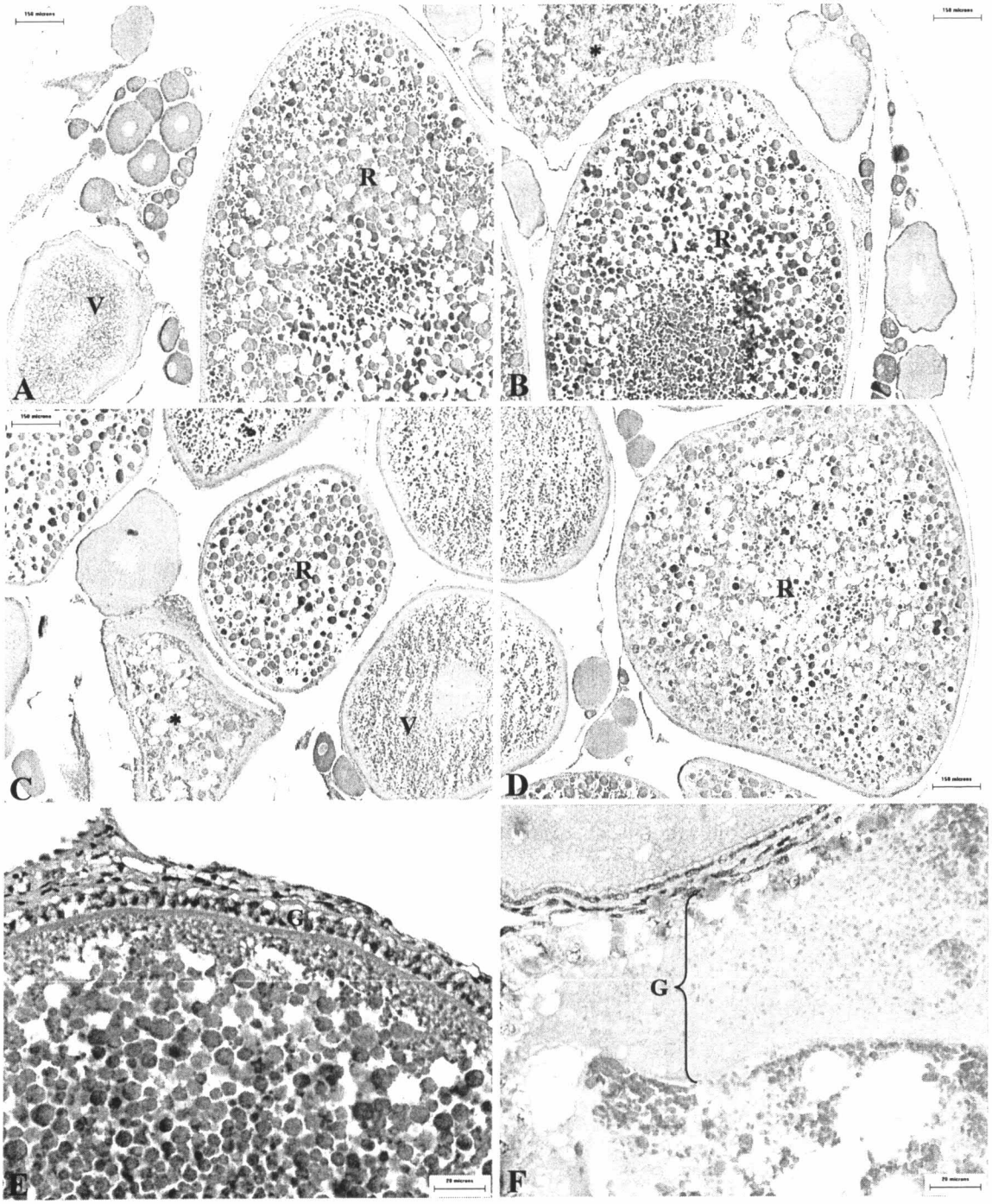

Figure 4-8: Mature ovaries of *O. niloticus* at 7 months post-exposure. (A-B) Control ovary shows large ripe oocytes. *Bar*: 150 μm. (C-D) Treated ovary shows large ripe oocytes and atretic follicle (*). *Bar*: 150 μm. (E) Follicle of ripe oocyte of the control fish shows thin granulosa and thecal cell layers. *Bar*: 20 μm. (F) Follicle of ripe oocyte of the treated fish with normal characters as the control. *Bar*: 20 μm.

R ripe oocyte, *G* granulosa cell, *T* thecal cell.

Figure 4-8

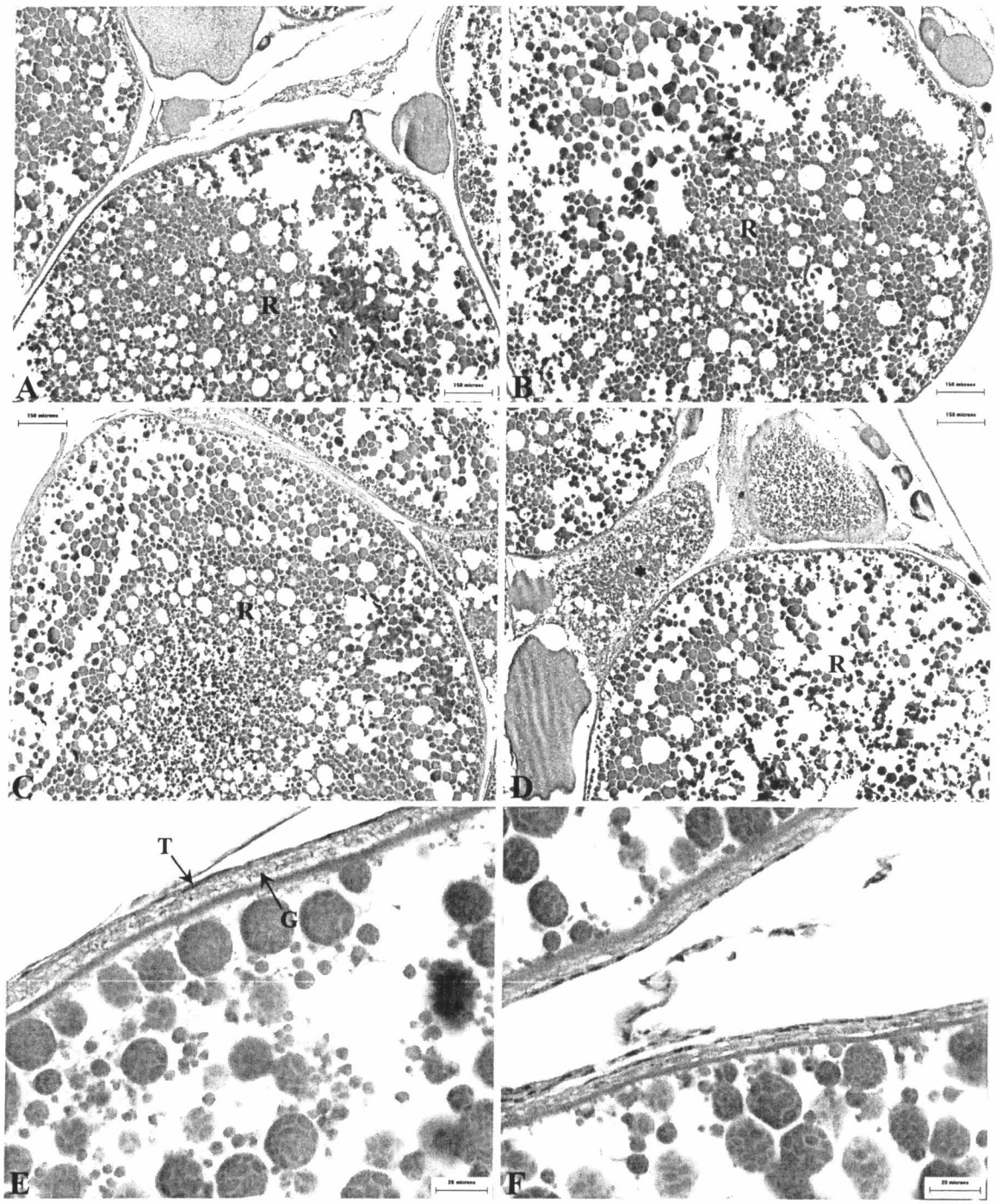

Figure 4-9: Electron micrograph of ovarian follicles of the control *O. niloticus*. (A) Follicle of perinucleolar oocyte with squamous granulosa and thecal cell layers. ×10,000. *Bar*: 500 nm. (B) Follicle of cortical alveolar oocyte with thin vitelline envelope (arrow). ×5,000. *Bar*: 1 μm. (C) Follicle of vitellogenic oocyte with thick proliferated granulosa cell layer. Note the electron-dense materials (arrows) in granulosa cells and in ooplasm. ×5,000. *Bar*: 1 μm. (D) Follicle of ripe oocyte with thick vitelline envelope and simple layer of cuboidal granulosa cells. ×3,000. *Bar*: 2 μm.

O oocyte, *Ve* vitelline envelope, *G* granulosa cell, *Bm* basement membrane, *T* thecal cell.

Figure 4-9

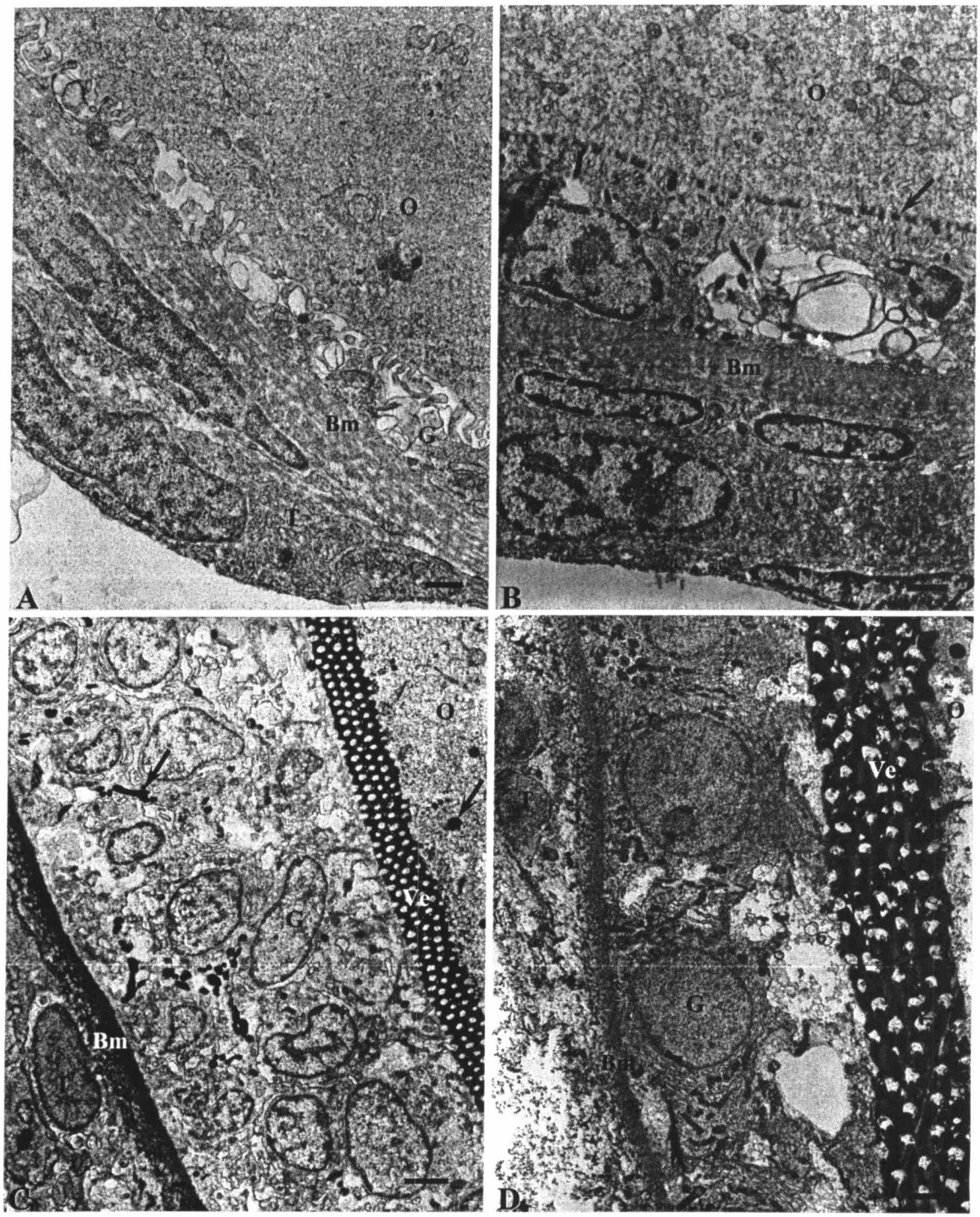

Figure 4-10: Electron micrograph of ovarian follicles of the treated *O. niloticus*. (A) Follicle of perinucleolar oocyte with squamous granulosa cells and cytoplasm-rich thecal cells. ×5,000. *Bar*: 1 μm. (B) Follicle of cortical alveolar oocyte with thin vitelline envelope and electron-dense material in granulosa and thecal cell layer (arrows). ×5,000. *Bar*: 1 μm. (C) Follicle of vitellogenic oocyte with hypertrophied granulosa cell layer. ×3,000. *Bar*: 2 μm. (D) Follicle of ripe oocyte with abnormal homogeneous layer of the vitelline envelope (*). ×4,000. *Bar*: 2 μm.

O oocyte, *Ve* vitelline envelope, *G* granulosa cell, *Bm* basement membrane, *T* thecal cell.

Figure 4-10

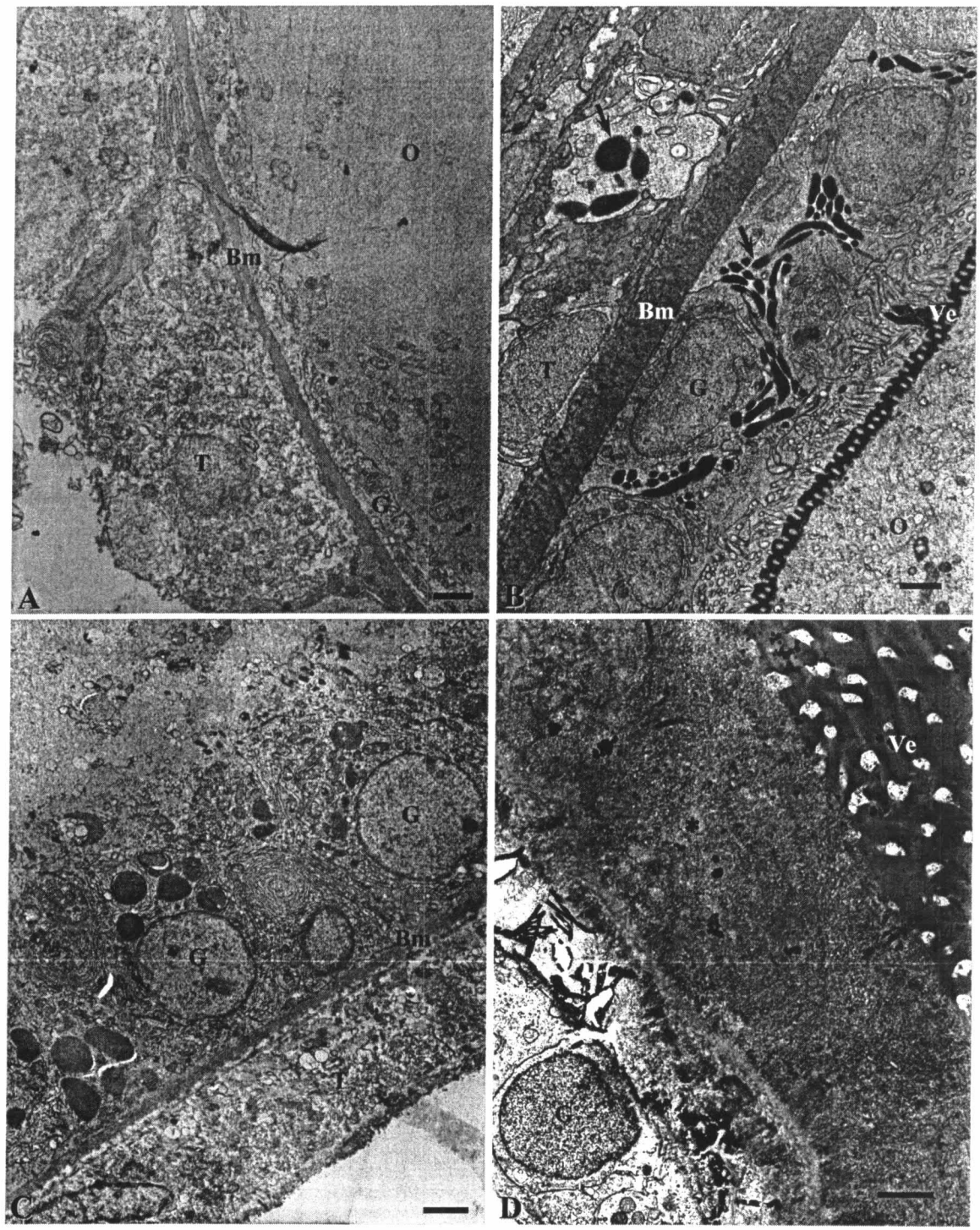

Figure 4-11: Electron micrograph of granulosa cells of the control *O. niloticus*. (A) Granulosa cell of perinucleolar oocyte with microvilli contacted with the oocyte and multivesicular bodies. ×20,000. *Bar*: 200 nm. (B) Granulosa cell of cortical alveolar oocyte with deposition of some electron-dense material (*). Note the interdigitation of microvilli with deposition of electron-dense material forming visible vitelline envelope. ×20,000. *Bar*: 200 nm. (C) Granulosa cell of vitellogenic oocyte with numerous mitochondria, dilated tubular RER, free ribosomes (square) and electron-dense material (*). ×20,000. *Bar*: 200 nm. (D) Granulosa cell of ripe oocyte with abundant elongate mitochondria, RER and free ribosomes (square). ×15,000. *Bar*: 500 nm.

O oocyte, *Bm* basement membrane, *N* nucleus, *RER* rough endoplasmic reticulum, *m* mitochondria, *mvb* multivesicular bodies, *mv* microvilli.

Figure 4-11

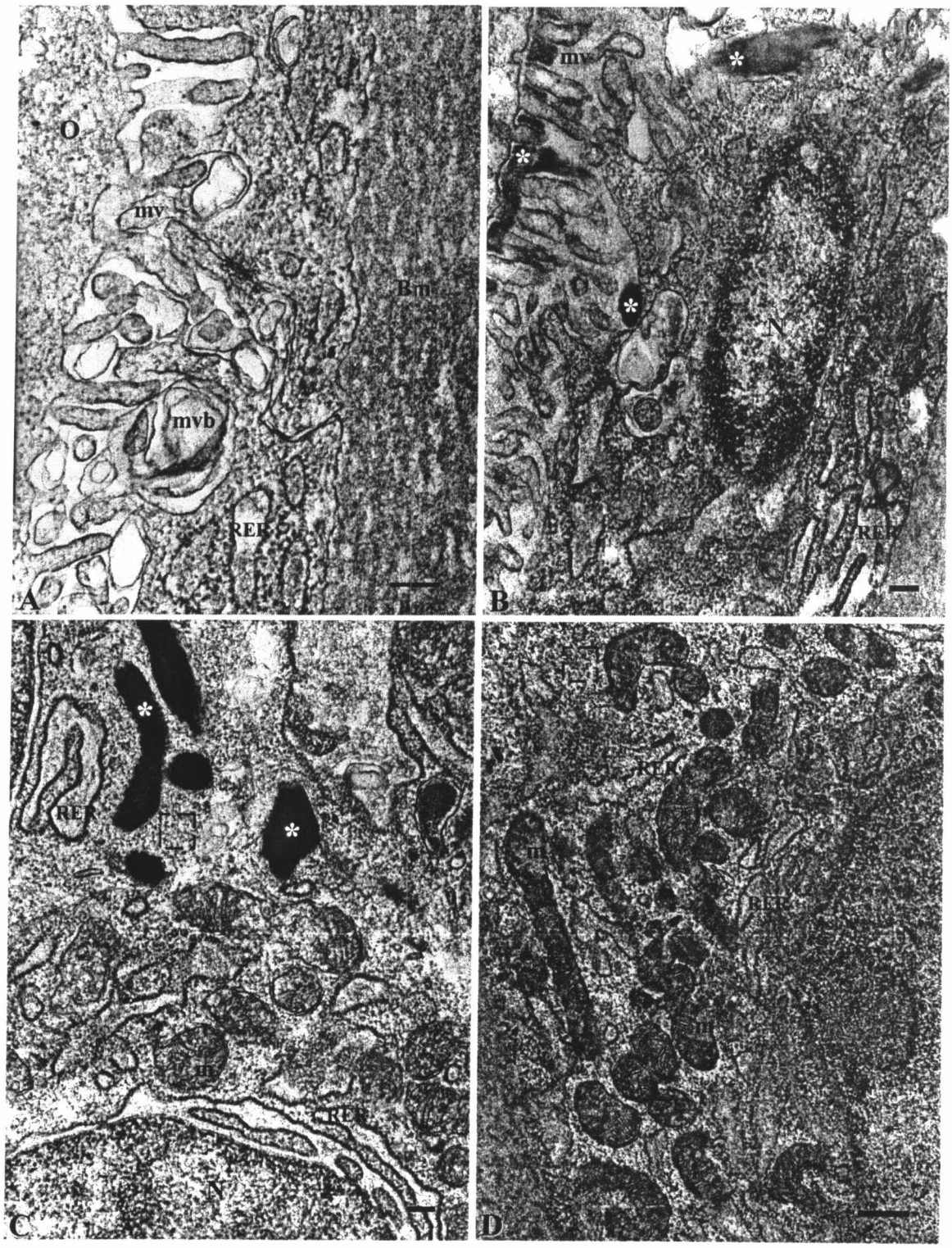

Figure 4-12: Electron micrograph of granulosa cells of the treated *O. niloticus*. (A) Granulosa cell of perinucleolar oocyte. ×20,000. *Bar*: 200 nm. (B) Granulosa cell of cortical alveolar oocyte with well developed Golgi system, RER and deposition of electron-dense material. ×20,000. *Bar*: 200 nm. (C) Granulosa cell of vitellogenic oocyte with hypertrophied granulosa cell layer. All organelles are packed in the periphery near the basement membrane including RER whorl. ×8,000. *Bar*: 1 μm. (D) Granulosa cell of ripe oocyte with spherical mitochondria, lipid droplets and transport vesicles. ×15,000. *Bar*: 500 nm.

O oocyte, *Ve* vitelline envelope, *G* granulosa cell, *Bm* basement membrane, *N* nucleus, *g* Golgi system, *RER* rough endoplasmic reticulum, *m* mitochondria, *mvb* multivesicular bodies, *mv* microvilli, *l* lipid vesicle, *v* transport vesicle.

Figure 4-12

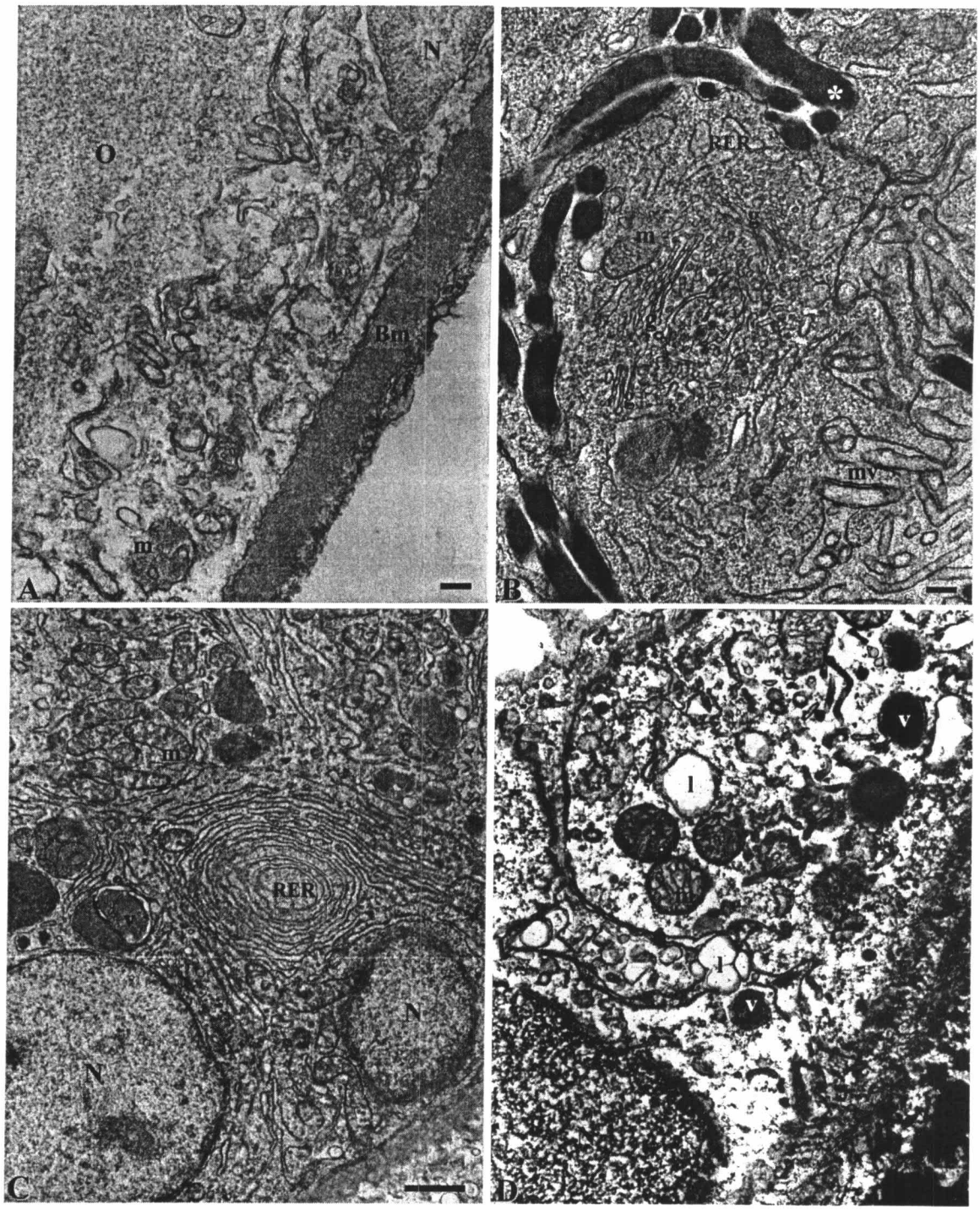

Figure 4-13: Electron micrograph of thecal cells of the control *O. niloticus*. (A) Thecal cell of perinucleolar oocyte with abundant globular SER (arrows). ×40,000. *Bar*: 200 nm. (B) Thecal cell of cortical alveolar oocyte. Mitochondria with tubulovesicular cristae, SER (arrows) and transport vesicles are seen. ×20,000. *Bar*: 200 nm. (C) Thecal cell of vitellogenic oocyte with abundant round-oval mitochondria with tubulovesicular cristae (arrowheads), elongated mitochondria with lamellar cristae and abundant globular SER (arrows). ×20,000. *Bar*: 200 nm.

N nucleus, *m* mitochondria, *v* transport vesicle.

Figure 4-13

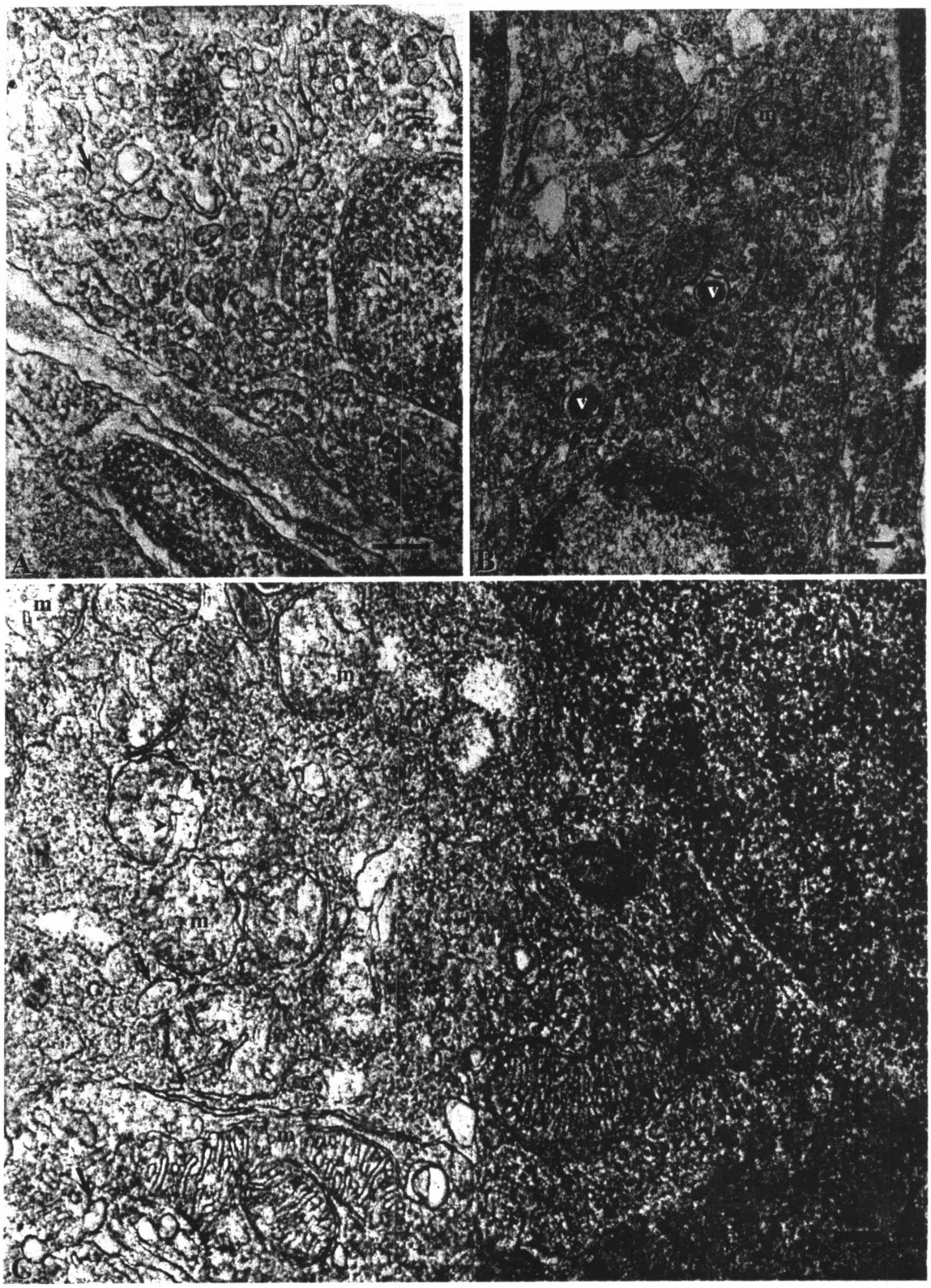

Figure 4-14: Electron micrograph of thecal cells of the treated *O. niloticus*. (A) Thecal cell of perinucleolar oocyte with abundant mitochondria and globular SER. ×20,000. *Bar*: 200 nm. (B) Thecal cell of cortical alveolar oocyte shows myelin figures and dilated ER. ×20,000. *Bar*: 200 nm. (C) Thecal cell of vitellogenic oocyte. Note the abundant of elongated mitochondria with tubular cristae (arrowheads) and abundant SER. ×20,000. *Bar*: 200 nm.

N nucleus, *dER* dilated endoplasmic reticulum, *RER* rough endoplasmic reticulum, *m* mitochondria, *my* myelin figures, *v* transport vesicle.

Figure 4-14